









Isotope-labeled amyloid- β does not transmit to the brain in a prion-like manner after peripheral administration

Mirjam Brackhan^{1,2} , Giulio Calza³, Kristiina Lundgren³, Pablo Bascuñana¹ , Thomas Brüning¹ , Rabah Soliymani³ , Rakesh Kumar⁴ , Axel Abelein⁴ , Marc Baumann³, Maciej Lalowski³  & Jens Pahnke^{1,2,5,*} 

Abstract

Findings of early cerebral amyloid- β deposition in mice after peripheral injection of amyloid- β -containing brain extracts, and in humans following cadaveric human growth hormone treatment raised concerns that amyloid- β aggregates and possibly Alzheimer's disease may be transmissible between individuals. Yet, proof that A β actually reaches the brain from the peripheral injection site is lacking. Here, we use a proteomic approach combining stable isotope labeling of mammals and targeted mass spectrometry. Specifically, we generate ¹³C-isotope-labeled brain extracts from mice expressing human amyloid- β and track ¹³C-lysine-labeled amyloid- β after intraperitoneal administration into young amyloid precursor protein-transgenic mice. We detect injected amyloid- β in the liver and lymphoid tissues for up to 100 days. In contrast, injected ¹³C-lysine-labeled amyloid- β is not detectable in the brain whereas the mice incorporate ¹³C-lysine from the donor brain extracts into endogenous amyloid- β . Using a highly sensitive and specific proteomic approach, we demonstrate that amyloid- β does not reach the brain from the periphery. Our study argues against potential transmissibility of Alzheimer's disease while opening new avenues to uncover mechanisms of pathophysiological protein deposition.

Keywords Alzheimer's disease; brain; multiple reaction monitoring immunomass spectrometry; prion-like; seeding

Subject Categories Molecular Biology of Disease; Neuroscience

DOI 10.15252/embr.202154405 | Received 30 November 2021 | Revised 30 April 2022 | Accepted 3 May 2022 | Published online 27 May 2022

EMBO Reports (2022) 23: e54405

Introduction

Cerebral deposition of amyloid- β (A β), a cleavage product of the amyloid precursor protein (APP), is thought to be integral to the pathogenesis of Alzheimer's disease (AD; Hardy & Higgins, 1992; Selkoe, 2001). A β can form aggregates that expose their surface structure to soluble monomeric A β peptides leading to conformational adaption and growing agglomerates (Cohen *et al*, 2013; Meisl *et al*, 2014). It was shown in pre-depositing APP-transgenic (tg) mice that intraperitoneal (i.p.), intravenous, intramuscular, and intraocular administration of A β -containing brain extract from aged APPtg donor mice or AD patients accelerate A β deposition in the meninges and brain, suggesting that A β or its so-called seeds may be transported from the periphery to the brain (Eisele *et al*, 2010, 2014; Burwinkel *et al*, 2018; Morales *et al*, 2021). In the absence of proven transmissibility (Eisele, 2013; Irwin *et al*, 2013; Asher *et al*, 2020), these findings were denoted as prion-like properties of A β (Jucker & Walker, 2013). Similarly, early cerebral A β deposition was reported in around 50% of the individuals in cohorts that had received treatment with cadaveric human growth hormone (c-hGH) during childhood and died of iatrogenic Creutzfeldt-Jakob disease or other causes at a young age (Jaunmuktane *et al*, 2015; Ritchie *et al*, 2017; Cali *et al*, 2018). Certain c-hGH batches used to treat these patients were shown to contain A β and to accelerate A β deposition in the brains of APP-knockin mice after intracerebral injection (Purro *et al*, 2018). These findings raised concern that A β pathology and possibly AD may be transmissible between humans. However, another study found evidence of cerebral β -amyloidosis in only 1 of 24 iatrogenic Creutzfeldt-Jakob disease cases following c-hGH treatment even though A β was present in various hGH batches used for the treatment (Duyckaerts *et al*, 2018).

In general, it remains contentious whether cerebral β -amyloidosis was induced by seeding from the periphery or by other

1 Department of Pathology, Section of Neuropathology, Translational Neurodegeneration Research and Neuropathology Lab, University of Oslo and Oslo University Hospital, Oslo, Norway

2 LIED, University of Lübeck, Lübeck, Germany

3 Meilahti Clinical Proteomics Core Facility, Faculty of Medicine, Helsinki Institute of Life Science, University of Helsinki, Helsinki, Finland

4 Department of Biosciences and Nutrition, Karolinska Institute, Huddinge, Sweden

5 Department of Pharmacology, Faculty of Medicine, University of Latvia, Riga, Latvia

* Corresponding author. Tel: +47 230 71466; E-mail: jens.pahnke@gmail.com

causes. Underlying neuroendocrine disorders in c-hGH recipients (Adams *et al*, 2016; Feeney *et al*, 2016) or inflammatory stimuli in the A β -containing brain extract injected into mice could also exacerbate A β pathology as shown for peripheral injection of lipopolysaccharides in APPTg mice (Wendeln *et al*, 2018). Moreover, A β from donor mice is not biochemically or histologically differentiable from endogenous A β in injected host mice, leaving the interpretation that A β indeed entered the brain from the periphery speculative. To overcome this key limitation, we combined stable isotope labeling of donor brains and highly sensitive multiple reaction monitoring immuno-mass spectrometry (MRM-IMS). This approach enabled us to investigate whether brain-derived, labeled A β reaches the brain from the periphery.

Results and Discussion

Labeling of donor brains

To generate brain extracts containing labeled A β that can be differentiated from endogenous A β in injected host mice without altering

its chemical or conformational characteristics, we fed APPTg mice (APP/PS1, a model featuring early onset of A β pathology at 6–8 weeks of age; Radde *et al*, 2006) a diet containing the fully ^{13}C -substituted version of lysine (^{13}C -Lys, 6 additional neutrons; Kruger *et al*, 2008), starting at 50 or 75 days of age with different feeding durations (Table 1). We assessed the labeling efficiency and concentration of A β by mass spectrometry (MS) and immunoassay, respectively (Fig 1A). The percentage of ^{13}C -Lys-labeled A β increased with both longer feeding duration (50 vs. 125 days of feeding, $P < 0.0001$) and earlier commencement of feeding (start at 50 vs. 75 days of age, $P < 0.0001$, Fig 1B–D, Table 1). Correspondingly, the absolute concentration of ^{13}C -Lys-labeled A β increased with longer feeding duration. Interestingly, the absolute concentration of unlabeled A β was 5.0 ± 1.3 ng/mg brain when feeding started at 75 days of age, and 1.7 ± 0.3 ng/mg brain when commenced at 50 days of age, independent of the total feeding time. This implies that approximately 3 ng A β /mg brain were newly generated between the ages of 50 and 75 days and that insoluble A β that had been generated when labeling started was not subject to dynamic turnover (Fig 1E). Additionally, overall labeling efficiency was assessed by MS in four mice labeled from 50–150 days of age,

Table 1. ^{13}C -Lys-labeling of APPTg donor brains for ^{13}C -Lys APPTg brain extract generation.

Animal ID	Age (days)	^{13}C -Lys diet (days)	ng A β 42/mg brain	Ratio ^{13}C -Lys/ unlabeled A β 17-28	% ^{13}C -Lys A β 17-28	Brain extract cohort
19290	125	75–125	11.9	1.4	57.6	1
19291	175	75–175	10.5	2.9	74.5	1
19293	175	75–175	21.7	2.4	70.2	1
19299	175	75–175	20.7	2.8	73.5	1
19300	175	75–175	20.1	2.7	72.9	1
19644	100	50–100	4.0	2.2	68.7	1
19646	100	50–100	5.2	2.5	71.8	1
19651	100	50–100	6.0	2.3	70.0	1
19696	100	50–100	5.3	2.5	71.4	1
19698	100	50–100	5.9	2.2	68.8	1
27279	175	50–175	12.6	8.8	89.8	2
27303	175	50–175	16.7	7.0	87.5	2
27324	175	50–175	18.9	7.2	87.8	2
27333	175	50–175	11.1	5.7	85.0	2
27335	175	50–175	13.1	8.0	88.9	2
27341	175	50–175	13.9	8.2	89.1	2
27380	175	50–175	13.9	8.3	89.3	2
27409	175	50–175	13.9	7.3	87.9	2
27410	175	50–175	16.1	7.0	87.5	2
35073	125	50–125	6.4	3.8	79.3	3
35074	125	50–125	6.5	4.1	80.4	3
36356	150	50–150	13.1	5.6	84.8	4
36359	150	50–150	13.3	5.4	84.3	4
36371	150	50–150	14.8	6.1	85.9	4
36373	150	50–150	10.8	5.8	85.3	4

Animal ID number, age at death, age during which ^{13}C -Lys-labeled diet was fed, amount of A β 42 per mg brain, ratio between ^{13}C -Lys A β 17-28 and unlabeled A β 17-28, labeling efficiency in %, cohort for ^{13}C -Lys APPTg brain extract injection.

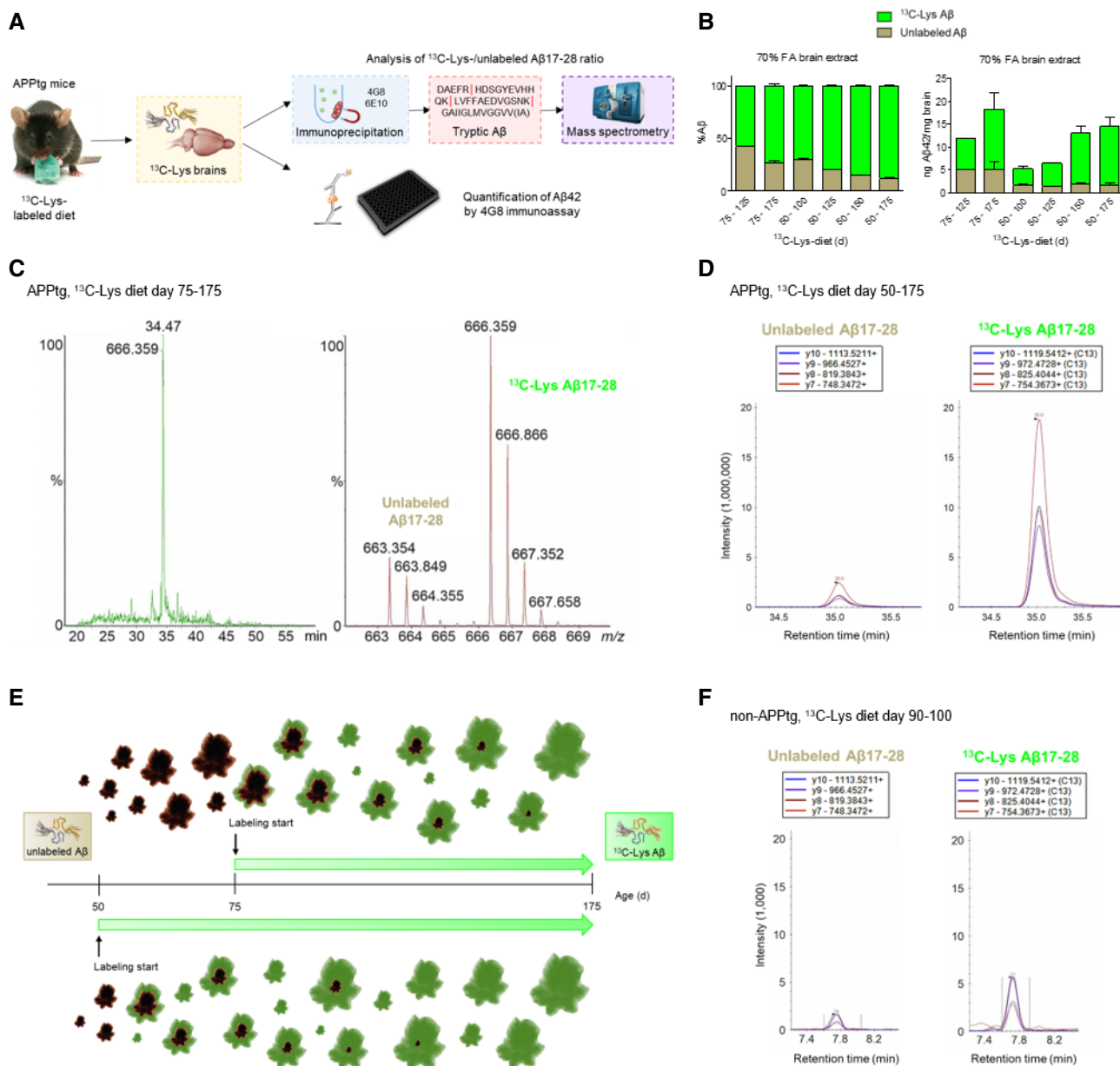


Figure 1. ¹³C-Lys-labeling of donor brains.

A Labeling strategy (image of mouse with diet provided by Cambridge Isotope Laboratories, Inc.) and quantification of ¹³C-Lys-labeled and unlabeled Aβ.
 B Relative (left) and absolute (right) amount of ¹³C-Lys-labeled and unlabeled Aβ in APPTg mouse brains after labeling from 75–125 days (*n* = 1), 75–175 days (*n* = 4), 50–100 days (*n* = 5), 50–125 days (*n* = 2), 50–150 (*n* = 4) or 50–175 days (*n* = 9) of age. Error bars show mean ± SD.
 C Representative chromatogram and mass spectra of doubly charged ions of unlabeled Aβ17-28 (663.3 m/z) and ¹³C-Lys Aβ17-28 (666.3 m/z) in an APPTg brain after labeling from 75–175 days. %- ion intensity, m/z- mass-to-charge. Data were acquired in data-independent analysis mode (MS⁵).
 D Representative chromatograms of unlabeled Aβ17-28 (left) and ¹³C-Lys Aβ17-28 (right) in an APPTg brain after labeling from 50–175 days. The intensities of four transitions (y10, y9, y8, and y7) were assessed. Data were acquired by MRM in nanoflow mode.
 E Illustration of ¹³C-Lys incorporation into Aβ depending on the starting point of labeling in APPTg mice. The later labeling starts, the higher is the amount of already generated, insoluble Aβ that is not metabolized anymore and consequently, not available for label incorporation. The earlier labeling starts, the higher is the fraction of newly produced Aβ incorporating the label.
 F Representative chromatograms of unlabeled Aβ17-28 (left) and ¹³C-Lys Aβ17-28 (right) in a non-APPTg brain after labeling from 90–100 days. Note the 1,000-fold difference in intensity magnitude between APPTg and non-APPTg brains. Data were acquired by MRM in microflow mode.

Source data are available online for this figure.

revealing $97.2 \pm 0.2\%$ overall ^{13}C -Lys-labeling of the brain proteome (Dataset EV1).

Brain homogenates were pooled into four cohorts (Table 1) and diluted to generate ^{13}C -Lys APPtg brain extracts with 2.9–6.2 ng total A β 42/ μl and 2.3–5.3 ng ^{13}C -Lys A β 42/ μl (Table EV1). To generate labeled negative controls (^{13}C -Lys non-tg extracts), non-APPtg mice received the ^{13}C -Lys-labeled diet for 10 days. We chose this labeling duration as the average life time of brain proteins had been reported to be 9 days (Price *et al.*, 2010). Mass spectrometry analysis of four mice revealed $83.3 \pm 2.9\%$ overall ^{13}C -Lys-labeling of the brain proteome (Dataset EV2) and detected minute signals of both unlabeled and ^{13}C -Lys A β 17–28 with an intensity $3\log_{10}$ lower (1/1,000) than in APPtg mice (Fig 1F), representing endogenous murine A β .

Moreover, unlabeled brain extracts for A β quantification in the periphery following i.p. injection were generated from APPtg and non-APPtg mice fed on an unlabeled standard diet throughout their lifespan. Analysis by immunoassay showed A β 42 concentrations ranging from 5.1 to 8.5 ng/ μl in unlabeled APPtg extracts (Tables EV1 and EV2), while A β 42 concentrations in non-tg extracts were below the detection limit. Additionally, we isolated A β 42 fibrils from unlabeled APPtg extract and tested their *in vitro* seeding activity by thioflavin T (ThT) fluorescence assay. A β 42 fibrils extracted from APPtg brain extract exerted a concentration-dependent seeding effect on A β 42 aggregation (Fig EV1A) whereas isolate generated from non-tg brain extract delayed A β 42 aggregation kinetics (Fig EV1B). Seeded A β 42 fibrils presented a heterogeneous morphology (Fig EV1C and D) while A β 42 fibrils aggregated without the presence of seeds displayed a more homogenous morphology (Fig EV1E).

The concept of protein tracking by labeling-based proteomics has been successfully employed by a recent study featuring *ex vivo* labeling of the mouse blood plasma proteome to investigate blood–brain transport of plasma proteins (Yang *et al.*, 2020). Our *in vivo* labeling approach not only generated labeled amyloidogenic brain material for peripheral injection of host mice but also revealed information on the deposition dynamics of A β in the brains of APPtg donor mice. The earlier labeling commences, the lower the amount of insoluble A β that is not subject to dynamic turnover, and the higher the label incorporation into A β , which highlights the importance of an early start of therapies promoting A β clearance. This observation is supported by a recent study combining stable isotope labeling with mass spectrometry imaging to monitor plaque growth in an APP-knockin mouse model and showing that label incorporation into A β is highest when labeling starts before plaque onset (Michno *et al.*, 2021).

Detection limit of MS methodology

Considering the possibilities that A β may enter the brain in very low amounts or does not reach the brain at all, we sought to use a highly sensitive MS methodology capable of detecting minute quantities of ^{13}C -Lys-labeled A β in brain samples. Aggregates of insoluble, full-length A β present in APPtg mouse brains are particularly prone to loss in chromatography columns and machinery (Yoo *et al.*, 2018). Thus, we combined an approach extracting both soluble and insoluble A β from APPtg mouse brains (Allue *et al.*, 2016) and trypsin digestion generating more readily detectable A β fragments (Bateman

et al., 2006). First, we performed trypsin digestion of synthetic A β 42 and analyzed the resulting peptides. The A β 17–28 peptide, which contains Lys at position 28, was detected with the highest intensity (Fig 2A) in accordance with previous findings (Bateman *et al.*, 2006; Kim *et al.*, 2014) and thus, was selected as a surrogate to measure total A β levels. Next, we analyzed the fragmentation pattern of unlabeled A β 17–28 (0 additional neutrons) and $^{13}\text{C}_6^{15}\text{N}_2$ -lysine ($^{13}\text{C}^{15}\text{N}$ -Lys) A β 17–28 (eight additional neutrons), an internal standard well differentiable from both unlabeled and ^{13}C -Lys A β 17–28 (six additional neutrons), revealing several fragment ions of which the y ions $y4$ – $y10$ were detected with the highest intensity (Fig 2B). These ions were further analyzed by MRM for unlabeled, ^{13}C -Lys and $^{13}\text{C}^{15}\text{N}$ -Lys A β 17–28, and the transitions with the highest intensity— $y10$, $y9$, $y8$, and $y7$ —were selected for subsequent measurements. To assess the sensitivity of the MRM approach, we subjected decreasing quantities of $^{13}\text{C}^{15}\text{N}$ -Lys A β 42 to trypsin digestion followed by MRM analysis, revealing a detection limit of 25 amol in the injected volume (Fig 2C). Subsequently, we evaluated the quality of our sample processing by extracting soluble and insoluble A β from APPtg mouse brains, spiking decreasing amounts of $^{13}\text{C}^{15}\text{N}$ -Lys A β 42 into the insoluble fraction, and subjecting the samples to immunoprecipitation, trypsin digestion, and MRM analysis. Our $^{13}\text{C}^{15}\text{N}$ -Lys-labeled A β standard was still clearly detectable at the level of 50 amol in the injected volume despite all sample-processing steps and the presence of an excess of unlabeled endogenous A β (Fig 2D).

Intraperitoneally injected A β is detectable in the periphery long after injection

Having generated ^{13}C -Lys-labeled brain extracts and set up a reliable MS methodology for A β detection at attomolar levels, we now investigated the spatiotemporal distribution of peripherally injected A β . To this aim, we administered an i.p. injection of 200 μl ^{13}C -Lys APPtg brain extract or ^{13}C -Lys non-tg brain extract into 50-day-old APPtg (APP/PS1 mice; Radde *et al.*, 2006) and harvested the liver, spleen, mesenteric lymph nodes, and brain at 1, 3, 5, 7, 10, 25, 50, 75, or 100 days after injection as well as peritoneal cells at 1–10 days after injection (Fig 3A, Table 2). All experimental samples were spiked with known femtomolar quantities of $^{13}\text{C}^{15}\text{N}$ -Lys A β 42 prior to immunoprecipitation, serving as a quality control for sample processing and an internal standard.

Analysis of the liver, spleen, mesenteric lymph nodes, and peritoneal cells from ^{13}C -Lys APPtg brain extract-injected mice by MRM-IMS revealed detectable ^{13}C -Lys A β 17–28 and unlabeled A β 17–28 at abundance ratios comparable to the ^{13}C -Lys/unlabeled A β ratios observed in the APPtg donor brains (Fig 3B). The abundance of both peptides was highest at 1–3 days after i.p. injection and decreased over time in all investigated tissues, with low levels still detectable at 100 days in the liver, at 75 days in the spleen and at 50 days in the mesenteric lymph nodes. In the liver, A β -positivity was also recognizable by immunohistochemistry in perisinusoidal macrophages (Browicz-Kupffer cells) for up to 10 days after injection of ^{13}C -Lys APPtg brain extract but not ^{13}C -Lys non-tg brain extract (Fig EV2, images shown for 1 day after injection).

To quantify the amount of A β reaching peripheral tissues after i.p. injection, we administered 200 μl of unlabeled APPtg brain extract or non-tg brain extract into 50-day-old APPtg mice and

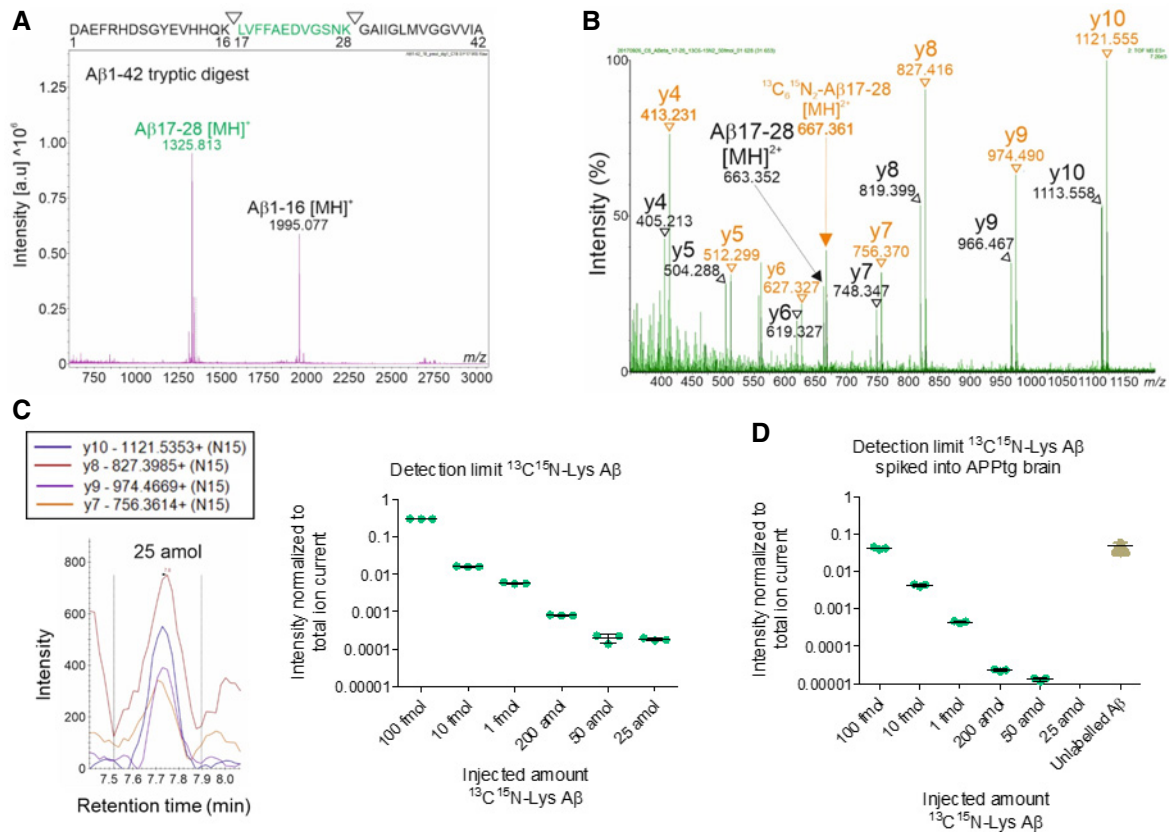


Figure 2. Detection limit of mass spectrometry methodology.

- A MALDI-TOF mass spectrum of trypsin-digested, synthetic A β 1-42 (10 pmol). The A β 17-28 [MH]⁺ fragment was detected with the highest intensity. Measurements in reflectron positive mode. The sequence of A β 1-42 with the tryptic cleavage sites is indicated at the top.
- B MS/MS spectrum of unlabeled A β 17-28 and ¹³C¹⁵N-Lys A β 17-28 synthetic peptides in the 50 fmol range. *m/z* of precursor ions (*m/z* 663.34 for A β 17-28 [MH]²⁺, *m/z* 667.36 for ¹³C¹⁵N-Lys A β 17-28 [MH]²⁺) and their derived fragments are indicated as a series of y ions (y4-y10). The peptides were analyzed in data-independent acquisition MS^E mode.
- C Decreasing quantities of synthetic ¹³C¹⁵N-Lys A β 1-42 were trypsin-digested and analyzed by MRM. The intensities of 4 transitions (y10, y9, y8, and y7) were assessed for ¹³C¹⁵N-Lys A β 17-28, showing a detection limit level of 25 amol. Measurements in technical triplicates, normalization to total ion current. Error bars show mean \pm SD.
- D Decreasing quantities of synthetic ¹³C¹⁵N-Lys A β 1-42 were spiked into the insoluble fraction of APPTg brains, immunoprecipitated, trypsin-digested, and analyzed by MRM. Assessment of the intensities of y10, y9, y8, and y7 showed a detection limit level of 50 amol for ¹³C¹⁵N-Lys A β 17-28 and detected an excess of brain-derived unlabeled A β 17-28. Measurements in technical triplicates, normalization to total ion current. Error bars show mean \pm SD.

Source data are available online for this figure.

harvested the liver, spleen, mesenteric lymph nodes, and peritoneal cells at 5 h, 1, 3, 5, 7, 10, 14, or 21 days after injection as well as blood at the time points 5 h to 7 days after injection. With immunoassay, we found A β 42 in the liver, spleen, mesenteric lymph nodes, and peritoneal cells of mice injected with APPTg brain extract until 21 days after injection (Fig 3C and D). In the liver, spleen, and mesenteric lymph nodes, A β 42 levels reached two peaks at 1 and 5 days after injection, with the liver accumulating most of the injected A β and the mesenteric lymph nodes the least (Fig 3D). In the peritoneal cells consisting predominantly of lymphocytes and to a lesser extent of macrophages and mesothelial cells, A β 42 levels were highest at 5 h after injection, with about half of the injected A β still being detectable, and subsequently decreased over time (Fig 3D). The decrease in A β observed over time in the liver and lymphoid tissues, suggests that A β does not replicate in the periphery and is in accordance with a previous study reporting that peripheral expression of

murine or human A β is not required for accelerating cerebral β -amyloidosis after i.p. injection of APPTg brain extracts (Eisele *et al*, 2014).

In blood plasma, A β 42 levels were comparable between mice injected with APPTg brain extract and those injected with non-tg brain extract at all time points (Fig EV3A). To further trace i.p. administered A β in blood, we isolated mononuclear blood cells, that is, lymphocytes and monocytes from mice injected with APPTg brain extract or non-tg brain extract at 5 h to 7 days after injection. We found higher levels of A β 42 in the APPTg brain extract-injected mice compared to non-tg brain extract-injected mice at 5 h and 1 day after injection, whereas A β 42 was only detectable in single individuals thereafter (Fig EV3B). The finding that injected A β is present in mononuclear blood cells but not in blood plasma during the first day after injection is in further concordance with the study by Eisele *et al* (2014). However, we cannot rule out that injected A β is present

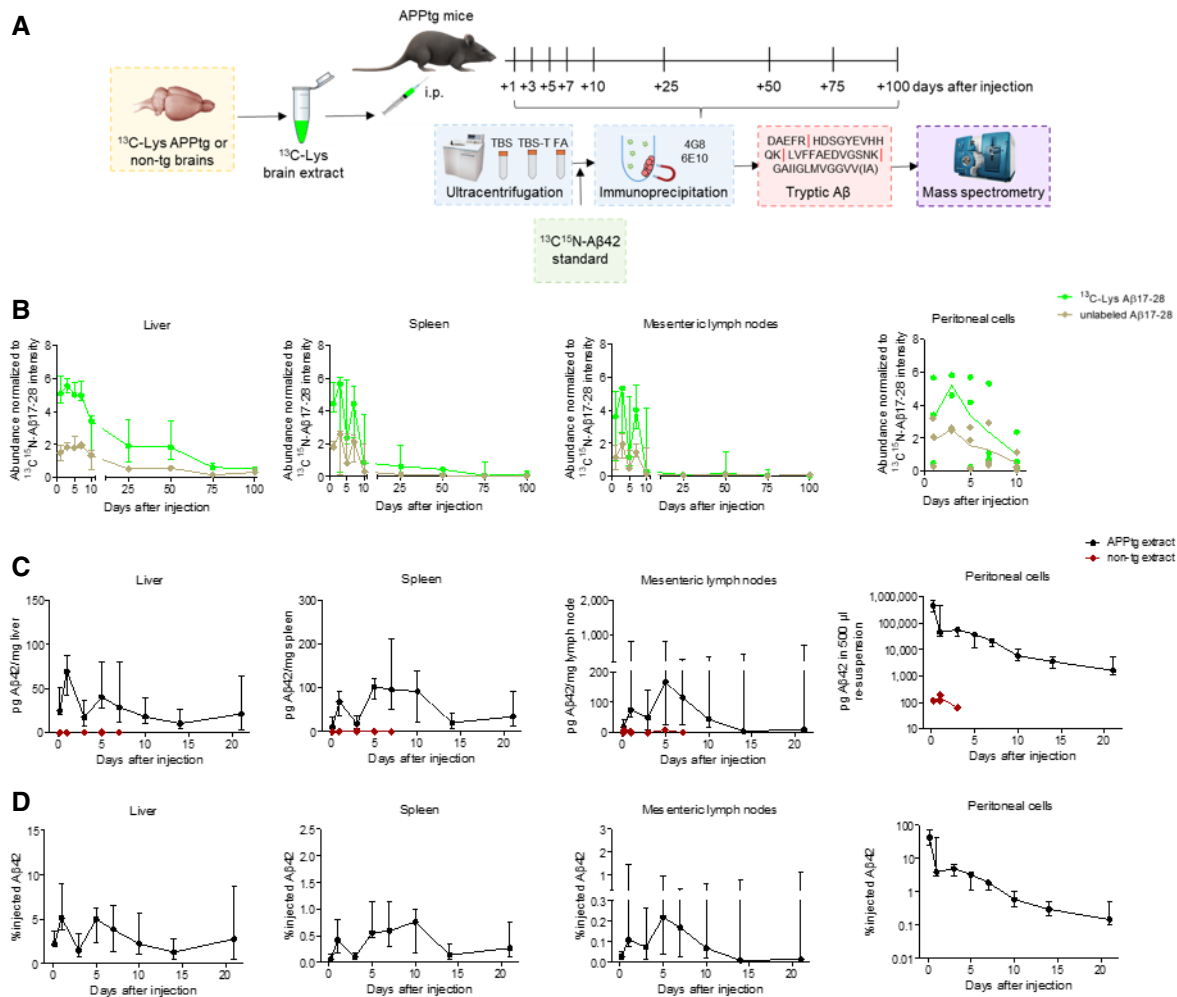


Figure 3. Intraperitoneally injected ^{13}C -Lys A β is detectable in the periphery long after injection.

A Experimental design. i.p., intraperitoneal.

B Temporal MRM analysis of ^{13}C -Lys A β 17-28 and unlabeled A β 17-28 in the liver, spleen, mesenteric lymph nodes, and peritoneal cells after ^{13}C -Lys-APPTg brain extract i.p. injection ($n = 3$ mice per time point and tissue at 1–10 days, except for $n = 2$ mice for peritoneal cells at 3 days; $n = 4$ mice per time point and tissue at 25–100 days, except for $n = 3$ mice for spleen at 100 days). Measurements in technical triplicates, normalization to $^{13}\text{C}^{15}\text{N}$ -Lys A β 17-28 intensity as a spiked internal standard and additionally to organ weight (mg) for lymph nodes. Error bars show median \pm interquartile range.

C Temporal 4G8 immunoassay quantification of A β 42 in the liver, spleen, mesenteric lymph nodes, and peritoneal cells after unlabeled APPTg ($n = 8$ mice at 5 h to 7 days, except for $n = 5$ mice for peritoneal lavage, $n = 5$ mice at 10–14 days, $n = 4$ mice at 21 days) or non-tg brain extract injection ($n = 2$ mice at 5 h and 3 days, $n = 3$ mice at 1 day, $n = 1$ mouse at 5 and 7 days, except for peritoneal cells where $n = 1$ mouse at 5 h and 3 days, and $n = 2$ mice at 1 day). Error bars show median \pm interquartile range.

D Normalization of APPTg extract group data presented in (C) to organ weight (mg) and injected A β amount (range 1,027–1,426 ng). Error bars show median \pm interquartile range.

Source data are available online for this figure.

in blood plasma at levels below the detection limit of the immunoassay or that binding of A β to soluble transport proteins such as low-density lipoprotein receptor-related protein-1 (Sagare *et al*, 2007) leads to epitope masking, thereby reducing A β detection in the immunoassay.

Taken together, these data suggest that A β injected into the peritoneum first reaches the liver and spleen via mononuclear blood cells, and the mesenteric lymph nodes via lymphatic drainage. The second peak observed in the liver, spleen, and lymph nodes may be attributable to clearance of A β -loaded immune cells from the peritoneum.

Labeled A β is detectable in the brain after peripheral injection of both ^{13}C -Lys APPTg and ^{13}C -Lys non-tg brain extract due to incorporation of ^{13}C -Lys

Having traced i.p. injected A β in the periphery, we now sought to answer the central question whether A β entered the brain. Analysis of the soluble brain fraction by MRM-IMS did not detect ^{13}C -Lys A β 17-28 at any time point after injection of ^{13}C -Lys APPTg brain extract while unlabeled A β 17-28 was present in low abundance at all time points (Fig 4A). Surprisingly, we observed ^{13}C -Lys A β 17-28 already at 1 day after injection in the insoluble brain fraction of

Table 2. ¹³C-Lys brain extract injection groups.

<i>n</i>	Genotype	Injected ¹³ C-Lys brain extract	Labeling duration brain donors (days)	Time point post-injection (days)	Age (days)
3	APPtg	APPtg, cohort 1	50, 100	1	51
3	APPtg	non-tg	10	1	51
3	APPtg	APPtg, cohort 1	50, 100	3	53
3	APPtg	non-tg	10	3	53
3	APPtg	APPtg, cohort 1	50, 100	5	55
3	APPtg	non-tg	10	5	55
3	APPtg	APPtg, cohort 1	50, 100	7	57
3	APPtg	non-tg	10	7	57
3	APPtg	APPtg, cohort 1	50, 100	10	60
3	APPtg	non-tg	10	10	60
4	APPtg	APPtg, cohort 2	125	25	75
4	APPtg	non-tg	10	25	75
4	APPtg	APPtg, cohort 2	125	50	100
4	APPtg	non-tg	10	50	100
4	APPtg	APPtg, cohort 2	125	75	125
4	APPtg	non-tg	10	75	125
3	APPtg	APPtg, cohort 1	50, 100	100	150
1	APPtg	APPtg, cohort 2	125	100	150
4	APPtg	non-tg	10	100	150
6	APPtg	APPtg, cohort 4	100	1	51
6	APPtg	non-tg	100	1	51
3	non-APPtg	APPtg, cohort 3	75	1	51

n = number of animals, genotype of injected animals, injected brain extract, number of days during which the donors of brains used for extract generation had received the ¹³C-Lys diet, sacrifice time point after injection, age at death.

both groups of mice, injected either with ¹³C-Lys APPtg brain extract or with ¹³C-Lys non-tg brain extract (Fig 4B). The abundance of ¹³C-Lys Aβ17-28 was significantly higher in the ¹³C-Lys APPtg brain extract-injected group compared to the ¹³C-Lys non-tg brain extract-injected group between 1 and 25 days after injection (Fig 4B). Unlabeled Aβ17-28 was detected in the insoluble brain fraction with an abundance 1,000-fold higher than that of ¹³C-Lys Aβ17-28, steadily increasing over time without differences between the experimental groups (Fig 4C). In accordance with this, we did not find differences between groups at any time point when quantifying total cerebral

Aβ load by immunoassay at 1–100 days after injection (Fig 4D), and immunohistochemistry at 25–100 days after injection (Fig EV4A). Similarly, we did not observe group differences in microglial activation as assessed by immunohistochemistry 25–100 days after injection (Fig EV4B). To evaluate potential long-term effects, we administered an i.p. injection of 200 μl unlabeled APPtg or non-tg brain extract into 50-day-old APPtg mice and harvested the brain at 240 days after injection. Quantification of total cerebral Aβ load by immunoassay did not reveal differences between groups (Fig EV5). These results indicate that cerebral β-amyloidosis and concurrent neuroinflammation are not accelerated by i.p. injection of Aβ-containing brain extract in the APPtg model used in our study.

To explain the presence of increasing amounts of ¹³C-Lys Aβ17-28 in the ¹³C-Lys non-tg brain extract-injected group and to investigate whether the higher ¹³C-Lys Aβ17-28 abundance in the ¹³C-Lys APPtg brain extract-injected group was due to brain penetration of Aβ or due to different labeling durations in APPtg and non-APPtg brain donor mice, we performed additional experiments. First, we probed for the presence of naturally occurring ¹³C-Lys Aβ17-28 in the insoluble brain fraction of unlabeled APPtg mice at the age of 50 days. We did not detect ¹³C-Lys Aβ17-28 in unlabeled mice (Fig 4E), thereby excluding naturally occurring ¹³C-Lys Aβ17-28 as an explanation and implying that metabolized ¹³C-Lys from labeled extract had been incorporated into endogenous Aβ. To confirm this, we fed the ¹³C-Lys-labeled diet to 50-day-old APPtg mice for 1 or 3 days and analyzed the insoluble brain fraction by MRM-IMS. We detected ¹³C-Lys Aβ17-28 accounting for an 8% of total Aβ17-28 already after 1 day of ¹³C-Lys-labeled diet (Fig 4F), demonstrating rapid incorporation of ¹³C-Lys into endogenous Aβ. Next, we fed non-APPtg mice the ¹³C-Lys labeled diet for 100 days to have the same labeling duration as for APPtg donor mice, resulting in 96.5 ± 0.2% overall ¹³C-Lys-labeling of the brain proteome (Dataset EV3). We administered an i.p. injection of 200 μl ¹³C-Lys APPtg brain extract or ¹³C-Lys non-tg brain extract generated from cohorts of donor mice with equal labeling duration into 50-day-old APPtg mice and harvested the brain at 1 day after injection (Table 2). Analysis of the insoluble brain fraction by MRM-IMS revealed the presence of ¹³C-Lys Aβ17-28 at a comparable abundance in both groups, mice injected with ¹³C-Lys APPtg brain extract and those injected with ¹³C-Lys non-tg brain extract (Fig 4G). Taken together, these results indicate that the mice rapidly incorporated metabolized ¹³C-Lys, which is an essential amino acid, from the donor extracts into newly generated endogenous Aβ, whereas Aβ present in the APPtg donor extract did not enter the brain. Finally, non-APPtg mice injected with ¹³C-Lys APPtg brain extract (Table 2) showed substantially lower abundance of ¹³C-Lys Aβ17-28 at 1 day after injection (0.15 ± 0.09 relative to ¹³C¹⁵N-Lys Aβ17-28 abundance) compared to non-APPtg mice after 1 day of ¹³C-Lys diet (1.56 ± 0.29 relative to ¹³C¹⁵N-Lys Aβ17-28 abundance; Fig 4H), supporting the idea of a dose-dependent incorporation of ¹³C-Lys into murine Aβ rather than brain penetration of injected human Aβ.

Using *in vivo* stable isotope labeling of brain-derived Aβ and highly sensitive targeted MRM-IMS, we provide evidence that peripherally injected Aβ does not penetrate the brain but may be metabolized along with other labeled proteins, with the label being incorporated into newly generated Aβ. Thus, our findings argue against transmission of Aβ pathology via Aβ aggregates entering the brain from the periphery.

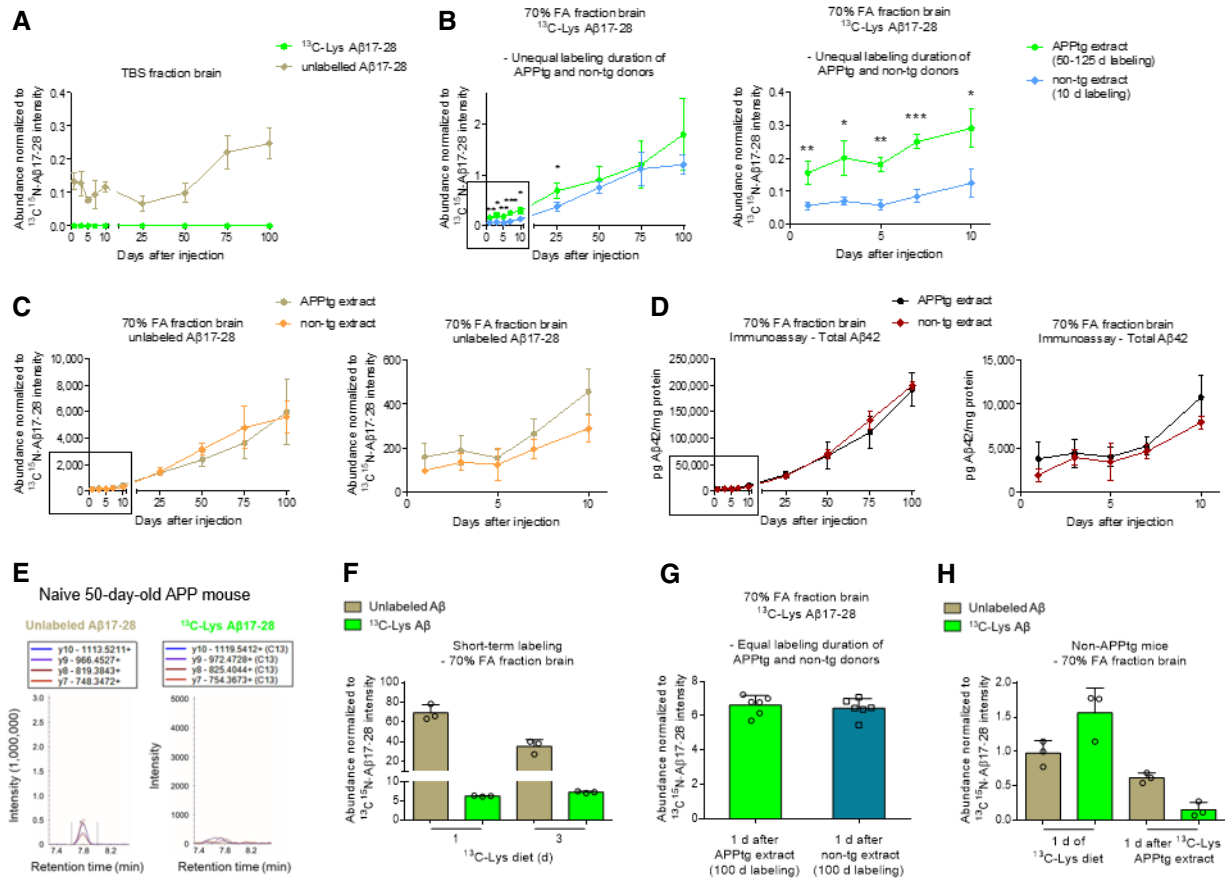


Figure 4. Insoluble ^{13}C -Lys A β is detectable in the brain after peripheral injection of both ^{13}C -Lys APPTg and ^{13}C -Lys non-tg brain extract due to incorporation of ^{13}C -Lys.

- A Temporal MRM analysis of unlabeled A β 17-28 and ^{13}C -Lys A β 17-28 in the soluble brain fraction after ^{13}C -Lys APPTg brain extract i.p. injection ($n = 3$ mice per time point at 1–10 days, $n = 4$ mice per time point at 25–100 days).
- B, C Comparative MRM analysis of ^{13}C -Lys A β 17-28 (B) and unlabeled A β 17-28 (C) in the insoluble brain fraction after ^{13}C -Lys-APPTg brain extract (donors labeled for 50–125 days) and ^{13}C -Lys-non-tg brain extract (donors labeled for 10 days) i.p. injection ($n = 3$ mice per group and time point at 1–10 days, $n = 4$ mice per group and time point at 25, 50, 100 days, $n = 3$ mice in the APPTg extract group and $n = 4$ in the non-tg extract group at 75 days), right side zoom for time points 1–10 days. Unpaired two-tailed *t*-test * $P < 0.05$ ($P = 0.0129$ at 3 days, $P = 0.0156$ at 10 days, $P = 0.0109$ at 25 days), ** $P < 0.01$ ($P = 0.0091$ at 1 day, $P = 0.0011$ at 5 days), *** $P < 0.001$ ($P = 0.0006$ at 7 days), ^{13}C -Lys APPTg extract-injected vs. ^{13}C -Lys non-tg extract-injected for each time point.
- D Comparative 4G8 immunoassay quantification of A β 42 in the insoluble brain fraction after ^{13}C -Lys APPTg or ^{13}C -Lys non-tg brain extract i.p. injection ($n = 3$ mice per group and time point at 1–10 days, $n = 4$ mice per group and time point at 25–100 days), right side zoom for time points 1–10 days. Normalization to protein concentration.
- E Representative chromatograms of unlabeled A β 17-28 (left) and ^{13}C -Lys A β 17-28 (right) in the brain of an unlabeled 50-day-old APPTg mouse not injected with labeled brain extract. Note the absence of ^{13}C -Lys A β 17-28.
- F MRM analysis of unlabeled and ^{13}C -Lys-labeled A β 17-28 in APPTg mouse brains after ^{13}C -Lys-labeled diet for 1 or 3 days ($n = 3$ mice per time point).
- G Comparative MRM analysis of ^{13}C -Lys A β 17-28 in the insoluble brain fraction after ^{13}C -Lys APPTg and ^{13}C -Lys non-tg brain extract (all donors labeled for 100 days) i.p. injection ($n = 6$ mice per group).
- H MRM analysis of unlabeled and ^{13}C -Lys-labeled A β 17-28 in non-APPTg mouse brains after ^{13}C -Lys-labeled diet for 1 days ($n = 3$ mice) or at 1 days after ^{13}C -Lys-APPTg brain extract i.p. injection ($n = 3$ mice).

Data information: In (A–C) and (F–H), measurements in technical triplicates, normalization to $^{13}\text{C}^{15}\text{N}$ -Lys A β 17-28 intensity as a spiked internal standard and brain weight (mg). All error bars show mean \pm SD. Source data are available online for this figure.

However, our data pointed to cerebral incorporation of metabolized ^{13}C -Lys from the donor extract into endogenous A β from 1 day after injection in both APPTg mice and non-APPTg mice, which only express murine APP and produce substantially lower A β amounts compared to APPTg mice. Incorporation of labeled amino acids into A β plaques has previously been observed in an AD patient 8 days after injection of ^{13}C -labeled leucine (Wildburger *et al*, 2018). We

speculate that ^{13}C -Lys-containing proteins and peptides from the injected donor extract may be metabolized in the periphery, resulting in release of ^{13}C -Lys – an essential amino acid – into the bloodstream. From there, ^{13}C -Lys may be transported into the brain and used for *de novo* production of A β . While we observed incorporation of ^{13}C -Lys into insoluble A β , we did not detect ^{13}C -Lys A β in the soluble brain fraction at any time point. This discrepancy is

most likely attributable to the proportion of soluble to insoluble A β in our brain samples, with soluble unlabeled A β being detected with an abundance 1,000–10,000-fold lower than insoluble unlabeled A β . Given that this low abundance of soluble unlabeled A β was already close to the limit of detection and that insoluble ^{13}C -Lys A β was detected with an abundance 1,000-fold lower than insoluble unlabeled A β , the abundance of soluble ^{13}C -Lys A β would be below the limit of detection in our study.

In accordance with the MS data not pointing to brain penetration of A β , we did not observe an acceleration of cerebral A β deposition in APP/PS1 mice injected with APPtg brain extracts, not even at 8 months after injection, the incubation period reported in previous peripheral injection studies (Eisele et al, 2014; Morales et al, 2021). The APPtg brain extracts used for i.p. injection in our experiments had A β concentrations of 2.9–8.5 ng total A β 42/ μl . This is comparable to previous peripheral injection studies using APPtg brain extracts with A β concentrations of 10–20 ng/ μl and demonstrating that extract diluted 10-fold (i.e., containing 1–2 ng A β / μl) still accelerated cerebral A β deposition (Eisele et al, 2010, 2014) or estimating the amount of intraperitoneally injected A β to be 171.8 ng (corresponding to an A β concentration of 1.7 ng/ μl ; Morales et al, 2021). Thus, insufficiently high levels of injected A β can be excluded as a potential confounder in our study.

Our findings imply that accelerated cerebral β -amyloidosis previously observed after peripheral injection of A β -containing brain extract or blood into APPtg mouse models (Eisele et al, 2010, 2014; Burwinkel et al, 2018; Morales et al, 2020, 2021) was caused by other factors present in the donor material rather than by seeding from the periphery. Indeed, a peripheral injection of lipopolysaccharides exacerbated A β pathology in a similar fashion as an i.p. injection of APPtg brain extract in APP23 mice (Wendeln et al, 2018). Moreover, it has been shown that exposing young mice to the systemic milieu or plasma of aged mice resulted in cognitive impairment and decreased synaptic plasticity and vice versa (Villeda et al, 2011). However, we did not observe accelerated cerebral β -amyloidosis in our study. This discrepancy with previous studies may be explained by differences in the rate of A β deposition in the different APPtg models used as host mice. While APP23 and Tg2576 mice used in previous studies start depositing A β at 6–7 months (Sturchler-Pierrat et al, 1997) and 8–10 months (Kawarabayashi et al, 2001), respectively, APP/PS1 mice used in our study already show first A β deposits at 1.5 months (Radde et al, 2006), potentially masking any accelerated plaque formation caused by still unknown factors in the donor material. In contrast to our findings arguing against brain penetration of A β , a recent study demonstrated that human A β derived from APPtg mice entered and accumulated in the brain of non-APPtg mice after 12 months of parabiosis (Bu et al, 2018). However, parabiosis models cause severe pain and distress that might promote sterile inflammatory factors facilitating the entrance of A β into the brain. As most of the A β was found in or near blood vessels, it cannot be discarded that these findings are the result of a loss of blood-brain barrier integrity due to the severity of the experimental model.

Our study implying that A β does not penetrate the brain from the periphery provides evidence against the intensely discussed hypothesis that human transmission of A β seeds and potentially AD may occur by medical procedures not directly involving the central nervous system (Jucker & Walker, 2015; Huynh & Holtzman, 2018;

Purro et al, 2018; Asher et al, 2020; Lauwers et al, 2020; Lau et al, 2021). Further studies are warranted to confirm our findings and investigate alternative mechanisms (e.g. inflammatory factors) that may have induced cerebral β -amyloidosis and other AD-related pathologies after injection of c-hGH or A β -containing brain material, thereby gaining new insights into the pathogenesis of AD. In addition to arguing against the potential transmissibility of AD, our proteomic approach combining *in vivo* stable isotope labeling and highly sensitive MRM-IMS provides a framework for deciphering deposition dynamics of proteins associated with proteopathic diseases.

Materials and Methods

Animals

APP/PS1 transgenic (APPtg) mice co-expressing human amyloid precursor protein with the KM670/671NL mutation, and L166P-mutated presenilin 1 under the control of the Thy1 promoter were provided by the University of Tübingen (Radde et al, 2006) and maintained on a C57BL/6J background. APPtg mice and their non-transgenic littermates were housed in groups in open cages at 21–22°C under a 12/12-h light/dark cycle with free access to food and water. All animal experiments were in accordance with the guidelines of the European Directive 2013/63/EU and Norwegian national laws and were formally approved by regional authorities (reference number 11909). Data is reported in accordance with the ARRIVE guidelines.

Brain donor mice

Male and female APPtg donor mice ($n = 25$) received a commercial $^{13}\text{C}_6$ -lysine (^{13}C -Lys)-labeled diet (EURISO-TOP GmbH, Saarbrücken, Germany) from 75–175 days ($n = 4$), 75–125 days ($n = 1$ sacrificed at 125 instead of 175 days due to skin lesions), 50–100 days ($n = 5$), 50–125 days ($n = 2$), 50–150 days ($n = 4$) or 50–175 days ($n = 9$) of age. Male and female non-APPtg donor mice aged 90–98 days ($n = 19$) received the diet for 10 days until the age of 100–108 days. An additional cohort of female non-APPtg donor mice was fed on the diet from 50–150 days of age ($n = 4$). Mice were sacrificed by cervical dislocation and intracardially perfused with cold phosphate-buffered saline (PBS). The brain was removed without cerebellum and lower brainstem, snap-frozen, and stored at -80°C .

Assessment of concentration and labeling efficiency of A β

Thawed brains were individually homogenized for 30 s with four 2.8 mm ceramic beads (PreCellys[®], Peqlab, Germany) using a Speed-Mill PLUS homogenizer (AnalytikJena AG, Germany). Brain homogenates from APPtg mice (~15 mg per sample) were mixed with 10 μl cold 70% formic acid (FA)/mg brain, sonicated for 2×30 s (Branson Digital Sonifier SFX 150, 3.2 mm microtip, amplitude 70%, pulses of 1 s) on ice, incubated overnight at 4°C, and centrifuged at $16,000 \times g$ for 90 min at 4°C. Supernatants were neutralized with 19 volumes of neutralization solution (1 M Tris, 0.5 M Na₂HPO₄, 0.05% NaN₃), and further diluted for electrochemiluminescence-linked immunoassay.

Overall A β 42 levels were quantified using the V-PLEX Plus A β 42 Peptide (4G8) Kit (detection limit 0.156 pg/ml; quantification limit 2.50 pg/ml) and a MESO QuickPlex SQ120 imager (Mesoscale Discovery, USA) according to the manufacturer's instructions.

To determine the percentage of ^{13}C -Lys A β , brain homogenates from APPtg mice (~6–11 mg per sample) were mixed with 200 μl of cold 70% FA, sonicated on ice, and centrifuged at 30,000 $\times g$ for 5 min at 4°C. Supernatants were neutralized with 12 ml of PBS/2 M Tris (1:1 ratio) solution, pH 8.45, and immunoprecipitated overnight with monoclonal anti-A β antibodies, clones 4G8 and 6E10 (BioLegendTM) cross-linked to magnetic beads (2.5 μg of each antibody covalently coupled to 50 μl of Protein G Dynabeads, Invitrogen; Thermo ScientificTM). Bound A β peptides were eluted from the beads with 2 \times 50 μl of 5% FA and digested overnight with sequencing grade trypsin (Promega) in 20% acetonitrile (ACN)/50 mM ammonium bicarbonate (AMBIC). The tryptic A β peptides were desalted and concentrated through C18 reversed phase (RP) ZipTips (MilliporeTM), eluted thrice from the ZipTips with 50% ACN/0.1% trifluoroacetic acid (TFA), and dried under vacuum. Brain homogenates from four non-tg mice were processed identically.

Tryptic digests from the APPtg mice that had received the labeled diet from 75–125, 75–175, or 50–100 days of age were re-suspended in 5% ACN and injected into a nanoAcquity UPLC system equipped with a trapping column (5 μm Xbridge C8 RP, 180 μm \times 20 mm), followed by an analytical C8 RP column (1.7 μm BEH C8, 75 μm \times 250 mm). The digests were separated with a linear gradient of 3–85% of solution B (0.1% FA/ACN) for 60 min at a flow rate of 250 nl/min and a stable column temperature of 35°C. All samples were run in triplicates, with three blanks between runs. The tryptic samples were analyzed in data-independent analysis mode (MS^E) on a Synapt G2-S mass spectrometer (WatersTM) by alternating between low collision energy (6 V) and high collision energy ramp in the transfer compartment (20–45 V) and utilizing 1 s cycle time. The separated peptides were detected online with a mass spectrometer operated in positive, resolution mode in the range of m/z 50–2,000 amu. Human [Glu¹]-fibrinopeptide B (Sigma Aldrich, St. Louis, MO, USA) at 150 fmol/ μl in 25% ACN/0.1% FA solution at a flow rate of 300 nl/min applied every 30 s, was used for lock mass correction. Chromatograms were analyzed with Progenesis QI ProteomicsTM using a mouse FASTA library (UniProtKB/Swiss-Prot reviewed) spiked with the human A β sequence (release 2018.08.01 with 16,994 sequences), and using SILAC $^{13}\text{C}_6$ and oxidation (M) as variable modifications with one trypsin-missed cleavage allowed. Database searches were carried out with the ion accounting algorithm and using the following parameters: default peptide and fragment tolerance, maximum protein mass 250 kDa; minimum fragment ions matches per protein ≥ 7 ; minimum fragment ions matches per peptide ≥ 3 ; minimum unique peptide matches per protein ≥ 2 ; false discovery rate (FDR) $< 4\%$. The extracted ion chromatograms were generated and peak areas for all ^{13}C -Lys labeled and unlabeled A β peptides were obtained using MassLynx v.4.1 software. Both procedures produced a peak table used for subsequent calculations. The ratios of $^{13}\text{C}/^{12}\text{C}$ were calculated based on normalized intensities and assessing peak areas of ^{13}C -Lys-labeled and unlabeled A β 17–28 peptide (detected at [MH]⁺, [MH]2⁺ and [MH]3⁺ charge states).

In another set of experiments, tryptic digests from the APPtg mice that had received the labeled diet from 50–125, 50–150, or 50–

175 days of age and non-APPtg mice were re-suspended in 5% ACN and injected into a 6500+ QTrap – Eksigent nanoLC system (SCIEXTM). Tryptic peptides from APPtg mice labeled from 50–175 days were separated using an ACQUITY UPLC M-Class Symmetry C18 Trap column (5 μm , 180 μm \times 20 mm, WatersTM) and an ACQUITY UPLC M-Class Peptide CSH C18 analytical column (3.5 μm , 75 μm \times 250 mm, WatersTM) with a 60 min gradient of 3–35% ACN/0.1% FA at a flow of 300 nl/min (nanoflow mode). Tryptic peptides from APPtg mice labeled from 50–125 or 50–150 days and non-tg mice were separated using a YMC Triart C18 column (1.9 μm ; 15 cm \times 150 mm; YMC Separation technology, Japan) at a flow of 7 $\mu\text{l}/\text{min}$ (microflow mode) and a column heater kept at 30°C with a 15-min step-wise gradient method of 3–85% ACN/0.1% FA. The multiple reaction monitoring (MRM) approach was used to analyze the samples, selecting four transitions for ^{13}C -Lys-labeled and unlabeled A β 17–28 with the highest intensity (y_{10} , y_9 , y_8 , and y_7). Raw MRM data (as.wiff files) were exported to Skyline (MacCoss Lab Software v.19.1) for peak integration, normalization and abundance calculations.

Assessment of total ^{13}C -Lys incorporation into the brain

Brain homogenate samples (~11 mg per sample) from APPtg mice ($n = 4$, fed for 100 days on ^{13}C -Lys diet) and control non-APPtg mice ($n = 4$, fed for 10 days, and $n = 4$, fed for 100 days on ^{13}C -Lys diet) were processed utilizing a previously described 3-step ultracentrifugation method (Allue *et al*, 2016) generating the soluble Tris-buffered saline (TBS) fraction, the membrane-soluble TBS + 1% Triton X-100 (TBS-T) fraction, and the insoluble 70% FA fraction but with the modification of using 2 ml of TBS and TBS-T, respectively, and 200 μl of 70% FA. Protein concentration in TBS fractions was assessed with Bradford assay (Pierce). 10 μg of protein mixture was reduced with 5.6 mM DTT for 5 min at 95°C and then alkylated with 5 mM iodoacetamide for 30 min at RT. Trypsin solution (Promega, Mannheim, Germany) was added in a ratio of 1:50 w/w in 250 mM ammonium bicarbonate and incubated overnight at room temperature with shaking. Tryptic digests were purified using C18-reverse-phase ZipTipTM (Millipore). Dried peptide digest was resuspended in 1% trifluoroacetic acid and sonicated in a water bath for 1 min before injection.

Tryptic digests were analyzed in nano-LC-Thermo Q Exactive Plus Orbi-Trap MS as described by us before (Gholizadeh *et al*, 2021). 1 μg of peptides in each biological sample was separated by Easy-nLC system (Thermo Scientific) equipped with a reverse-phase trapping column Acclaim PepMapTM 100 (C18, 75 μm \times 20 mm, 3- μm particles, 100 \AA ; Thermo Scientific), followed by an analytical Acclaim PepMapTM 100 RSLC reversed-phase column (C18, 75 μm \times 250 mm, 2- μm particles, 100 \AA ; Thermo Scientific). The injected sample analytes were trapped at a flow rate of 2 $\mu\text{l}/\text{min}$ in 100% of solution A (0.1% FA). After trapping, the peptides were separated with a linear gradient of 120 min comprising 96 min from 3 to 30% of solution B (0.1% FA/80% ACN), 7 min from 30 to 40% of solution B, and 4 min from 40 to 95% of solution B. The resolution was set to 140,000 for MS scans and 17,500 for the MS/MS scans. Full MS scans were acquired in 350–1,400 m/z range, and the 10 most abundant precursor ions were selected for fragmentation with 30 s dynamic of exclusion time. Ions with 2⁺, 3⁺ and 4⁺ charge states were selected for MS/MS analysis. Secondary ions

were isolated with a window of 1.2 m/z. The MS automatic gain control target was set to 3×10^6 counts, whereas the MS/MS automatic gain control target was set to 1×10^5 . Dynamic exclusion was set with a duration of 20 s. The Normalized Collision Energy was set to 28 kJ/mol. Each sample run was followed by two empty runs to wash out any remaining peptides from the previous runs.

The raw files were analyzed by Proteome Discoverer (PD, version 2.4.0.305, Thermo Scientific). The identification of proteins was performed against the *cptac2_mouse_hcd_selected* mouse spectral library (24-11-2014, updated on 08-07-2018 from <https://chemdata.nist.gov/>; compatible with MSPepSearch node in PD) and UniProt mouse protein database (release 08-2020 with 17,033 entries spiked with human A β PP sequence), a tolerance level of 10 ppm for MS and 0.02 Da for MS/MS, and with two tryptic missed cleavages allowed. The carbamidomethylation of cysteines was set as a fixed modification, whereas $^{13}\text{C}_6$ -Lys, the oxidation of methionines and deamidation of asparagines and glutamines were set as variable modifications. A minimum length of six amino acids (one peptide per protein) was required for each peptide hit. The $^{13}\text{C}/^{12}\text{C}$ ratios were calculated taking into account the ratios of normalized intensities for identified proteins, detected as heavy ($^{13}\text{C}_6$ -Lys) and light forms ($^{12}\text{C}_6$ -Lys). The efficiency of ^{13}C -Lys labeling was assessed by utilizing the following equation: SILAC ratio = [ratio (H/L) \times 100]/[ratio (H/L) + 1]. Only proteins detected at FDR < 0.01 at all levels of protein confidence with ≥ 2 unique peptides were taken into account in the quantitative analyses.

Preparation of brain extracts

To generate ^{13}C -Lys-labeled APPTg brain extracts, ^{13}C -Lys APPTg brain homogenates were pooled into four cohorts, diluted with 1 μl PBS per mg brain, and sonicated for 3 \times 30 s on ice. Negative control ^{13}C -Lys non-tg brain extracts were prepared identically. Brain extracts were aliquoted and stored at -80°C until use.

Additional cohorts of unlabeled APPTg and non-tg brain extracts originating from 100 to 175-day-old APPTg ($n = 59$, Table EV2) and 115 to 175-day-old non-APPTg donor mice ($n = 34$), which had received a standard laboratory diet throughout their entire life, were generated in an identical manner. Samples of ^{13}C -Lys-labeled and unlabeled APP brain extracts were treated with nine volumes of 70% FA and overall A β 42 levels were measured as described above.

Fibril extraction from brain extracts

Fibrils were extracted using a modified method from a recent study (Kollmer *et al*, 2019). Unlabeled APPTg brain extract (300 μl) was diluted with an equal volume of Tris calcium buffer (20 mM Tris, 138 mM NaCl, 2 mM CaCl_2 , 0.1% NaN_3 , pH 8) and centrifuged at 21,000 g for 30 min. The pellet was re-suspended in 1 ml Tris calcium buffer and 50 μl of Collagenase (5 mg/ml) and 10 μl of DNase I were added. The solution was vortexed, incubated overnight at 37°C , and centrifuged at 21,000 g for 30 min. The pellet was dissolved in 1 ml wash buffer (50 mM Tris, 10 mM EDTA, pH 8) and 40 μl of 10% SDS was added. The solution was incubated at 37°C for 30 min and centrifuged. This step was repeated twice and two further washing steps of the pellet were performed in wash buffer without SDS. Finally, the pellet containing fibrils was dissolved in 50 μl of 20 mM sodium phosphate buffer, 0.2 mM

EDTA pH 8.0, and used for further experiments. Unlabeled non-tg brain extract was processed identically as control.

Dot blot assay

The concentration of A β in fibril extract was estimated from dot blot using A β 42 monomer as reference. Fibril extract generated from APPTg brain extract was sonicated and spotted on a nitrocellulose membrane in different volumes (1, 2, 3, and 4 μl , respectively). 4 μl of A β 42 in different concentrations (1, 2, 3, 6, and 8 μM , respectively) was spotted as standard. The membrane was air-dried, blocked with blocking buffer (intercept[®] blocking buffer, LI-COR, Lincoln, USA) and incubated overnight at 4°C with primary anti-A β antibody (6E10, anti-mouse, 1:5,000, BioLegend[™]). The membrane was washed thrice with PBS-T, followed by incubation with secondary anti-mouse antibody (IRDye 800 CW, 1:20,000, LI-COR) for 60 min at 25°C . The membrane was washed thrice with PBS-T and developed using Odyssey[®] DLx Imaging System. Blot analysis was performed for estimation of A β concentration using ImageJ.

Thioflavin T fluorescence assay

To test the seeding activity of fibrils extracted from APPTg brain extract, a Thioflavin T (ThT) fluorescence assay was performed. 20 μl of sodium phosphate buffer (20 mM, 0.2 mM EDTA, pH 8.0) containing 3 μM A β 42 and 10 μM ThT was added to 384-well plates along with different volumes (1, 2, 3, 5, 8, 10, and 20 μl , respectively) of isolate generated from APPTg or non-tg brain extracts. Excitation filter at 440 nm and emission filter at 480 nm were selected and fluorescence was recorded at quiescent conditions at 37°C using a fluorimeter (FLUOStar Galaxy from BMG Labtech, Offenberg, Germany). The fluorescence data were plotted with respect to time after subtracting the minimum fluorescence value for each sample from all data points.

Transmission electron microscopy

To visualize the morphology of seeded A β 42 fibrils at the aggregation kinetic end points, transmission electron microscopy (TEM) was performed. 5 μl of aggregated samples from 384-well plates were spotted on a 400 mesh formvar/carbon-coated copper grid. Samples were washed twice with 10 μl of MQ water and stained with 1% uranyl formate. TEM (FEI Tecnai 12 Spirit BioTWIN, operated at 100 kV) images were recorded using a 2 \times 2 k Veleta CCD camera (Olympus Soft Imaging Solutions, GmbH, Münster, Germany). For each sample, 10–15 images were taken at a magnification of 20,000 \times –43,000 \times .

Detection limit of mass spectrometry methodology

Peptides A β 1-40 and A β 1-42 (Sigma-Aldrich), A β 17-28, $^{13}\text{C}_6$ $^{15}\text{N}_2$ -lysine ($^{13}\text{C}^{15}\text{N}$ -Lys) A β 17-28 and $^{13}\text{C}^{15}\text{N}$ -Lys A β 1-42 (all amino acid-analyzed; JPT Peptide Technologies GmbH, Berlin-Germany[™]) were solubilised in 1,1,1,3,3,3-hexafluoroisopropanol (Sigma-Aldrich). The peptides were digested in 40% ACN/0.2 M AMBIC overnight at 37°C using trypsin at 1:1 stoichiometric ratio, and subsequently desalted and concentrated using C18 RP ZipTips. Digested A β 1-40 and A β 1-42 (10 pmol) were analyzed by MALDI-TOF in reflectron

positive mode (m/z 1,000–5,000 Da on UltrafleXtreme, Bruker™) using α -hydroxycinnamic acid as a matrix, and the well-detectable A β 17-28 peptide was selected for further experiments. Peptides A β 17-28 and $^{13}\text{C}^{15}\text{N}$ -Lys A β 17-28 were analyzed at 50 fmol in data-independent acquisition MS^E mode on a C8 RP nano-column (1.7 μm BEH C8, 75 μm \times 250 mm) with a linear gradient of 3–85% of solution B (0.1% FA/ACN), for 60 min at a flow rate of 250 nl/min and stable column temperature of 35°C. Subsequently, MRM analyses were carried out, initially detecting seven MRM transitions for each labeling status of the tryptic peptide (y_{10} , y_9 , y_8 , y_7 , y_6 , y_5 , and y_4 for unlabeled, ^{13}C -Lys and $^{13}\text{C}^{15}\text{N}$ -Lys internal standard) achieving a cycle time of 1.5 s. The four transitions with highest intensity (y_{10} , y_9 , y_8 , and y_7) were selected for further studies. Decreasing amounts of $^{13}\text{C}^{15}\text{N}$ -Lys A β 1-42 were trypsin-digested and concentrated to find the limit of detection (100 fmol down to 25 amol in the final injection volume). Samples were re-suspended in 5% ACN and 4 μl injected each time into a 6500+ QTrap- Eksigent system operating in microflow mode as described above.

Brains from APPtg mice were processed by the 3-step ultracentrifugation method (Allue *et al*, 2016) described above but with the modification of using 2 ml of each solvent. The 70% FA fraction was spiked with $^{13}\text{C}^{15}\text{N}$ -Lys A β 1-42 at decreasing concentrations to find the limit of detection (100 fmol down to 25 amol in the final injection volume). Spiked samples were neutralized, immunoprecipitated, digested and analyzed by MRM as described above.

Intraperitoneal injection and short-term labeling experiments

For all injection experiments, mice were randomly assigned to experimental groups assuring that littermates were equally distributed between groups. Sample sizes were informed by prior literature using similar peripheral injection experiments with unlabeled brain material and our previous experience.

Male 50-day-old APPtg mice were injected i.p. with 200 μl of ^{13}C -Lys APPtg brain extract (donors labeled for 50, 100 or 125 days) or ^{13}C -Lys non-tg brain extract (donors labeled for 10 days). Mice were sacrificed by ketamine/xylazine overdose (400 mg/kg ketamine, 40 mg/kg xylazine) and intracardially perfused with 20 ml of cold PBS 1, 3, 5, 7, 10, 25, 50, 75, and 100 days after injection ($n = 3$ –4 per time point and extract). Peritoneal lavage with 2 \times 5 ml cold PBS was performed before intracardial perfusion at the time points 1–10 days. The brain, mesenteric lymph nodes, the spleen, and the liver were removed. Both brain hemispheres were snap-frozen at time points 1–10 days while one hemisphere was snap-frozen and the other one stored in 4% paraformaldehyde at time points 25–100 days. Peripheral organs were snap-frozen after removal of a small segment that was stored in 4% paraformaldehyde. The recovered cell suspension from the peritoneal lavage was centrifuged at 300 g for 8 min at room temperature. The cell pellet was re-suspended in 500 μl PBS and snap-frozen. All frozen samples were stored at -80°C .

Further male and female 50-day-old APPtg mice were injected i.p. with 200 μl of unlabeled APPtg brain extract (sacrificed at 5 h, and 1, 3, 5, 7, 14, and 21 days after injection; $n = 4$ –8 per time point) or non-tg extract as negative controls (sacrificed at 5 h, and 1, 3, 5 and 7 days after injection; $n = 1$ –3 per time point). The liver, spleen, mesenteric lymph nodes, peritoneal cells (at each time point), and EDTA-anticoagulated whole-blood samples from the

caudal vena cava (at time points 5 h to 7 days) were collected. Ten microliters of resuspended peritoneal cells were air-dried overnight on Superfrost® Plus slides at room temperature. Slides were fixed in methanol for 5 min and subjected to Giemsa staining to identify the composition of the peritoneal cells. Blood samples were centrifuged at 2,000 g for 15 min at 4°C and plasma was collected. In a separate experiment, EDTA-anticoagulated blood was taken by intra-cardiac puncture ($n = 2$ –3 mice per time point at 5 h to 7 days after APPtg extract injection, $n = 1$ per time point at 5 h to 7 days after non-tg extract injection) and mononuclear cells were isolated from blood samples using Ficoll-Paque PREMIUM 1.084 (GE Healthcare) according to the manufacturer's instructions. All samples were snap-frozen and stored at -80°C .

Moreover, male and female 50-day-old APPtg mice were injected i.p. with 200 μl of unlabeled APPtg brain extract ($n = 12$) or non-tg brain extract ($n = 11$) and sacrificed as described above at 240 days after injection. The brain was harvested and one hemisphere was snap-frozen and the other one stored in 4% paraformaldehyde. All frozen samples were stored at -80°C .

Additional male 50-day-old APPtg mice either were injected i.p. with 200 μl of ^{13}C -Lys APPtg or non-tg brain extract (all donors labeled for 100 days) and sacrificed 1 day after injection ($n = 6$ per group) or received the ^{13}C -Lys-labeled diet following overnight fasting and were sacrificed after 1 or 3 days of labeling ($n = 3$ per time point). Age-matched non-APPtg mice either were injected i.p. with 200 μl of ^{13}C -Lys APPtg brain extract and sacrificed 1 day after injection ($n = 3$) or received the ^{13}C -Lys-labeled diet following overnight fasting and were sacrificed after 1 day of labeling ($n = 3$). Mice were sacrificed as described above and the brain was harvested. Both hemispheres were snap-frozen and stored at -80°C .

Detection of labeled and unlabeled A β by multiple reaction monitoring immuno-mass spectrometry

The liver and spleen from mice injected with ^{13}C -Lys APPtg brain extract were homogenized on ice. Liver and spleen homogenates (20 mg per sample), and mesenteric lymph nodes were mixed with 200 μl of cold 70% FA, sonicated on ice, and centrifuged at 25,000 $\times g$ for 90 min at 4°C. The supernatants were spiked at 200 μl with 1.25 fmol of $^{13}\text{C}^{15}\text{N}$ -Lys A β 1-42 and neutralized in 12 ml of PBS/2 M Tris solution. Peritoneal cell suspensions (cell pellet in 500 μl of PBS) were incubated with 1 ml of 100% FA and processed as the other peripheral tissues. The supernatant was spiked at 1.5 ml with 1.25 fmol of $^{13}\text{C}^{15}\text{N}$ -Lys A β 1-42 and neutralized in 50 ml of PBS/2 M Tris solution.

Brains from mice either injected with ^{13}C -Lys APPtg or non-tg brain extracts or labeled for 1 or 3 days as well as from unlabeled APPtg mice at 50 days of age ($n = 2$) were processed as described in detection limit of mass spectrometry methodology and the resulting fractions were stored at -80°C . The TBS fraction from mice injected with ^{13}C -Lys APPtg brain extract was spiked at 200 μl with 1.25 fmol of $^{13}\text{C}^{15}\text{N}$ -Lys A β 1-42 in 20 μl of 70% FA and neutralized with 1.2 ml of PBS/2 M Tris (1:1 ratio) solution, pH 8.45. The 70% FA fraction from all mice was spiked at 200 μl with 10 fmol of $^{13}\text{C}^{15}\text{N}$ -Lys A β 1-42 and neutralized in 12 ml of PBS/2 M Tris solution.

Spiked, neutralized samples were immunoprecipitated as described above. Eluted A β peptides were neutralized to pH 8.5 with

1 M AMBIC and enzymatically digested by the addition of 2.5 µg of trypsin in 50% acetonitrile. The digested peptide solution was dried, re-suspended in 0.1–1% TFA to bring to pH < 4, concentrated and desalted twice, utilizing C18 RP ZipTip cartridges (50 cycles of sample binding and Aβ peptide elution by 10 × 10 µl of 70% ACN). The resulting eluate was dried and stored at –20°C until analysis. Subsequent MRM analysis was carried out by detecting the 4 transitions with the highest intensity (y10, y9, y8 and y7) for each labeling status of the tryptic peptide (unlabeled, ¹³C-Lys and ¹³C¹⁵N-Lys internal standard), with a dwell time of 100 ms, and achieving a cycle time of 1.26 s. Samples were re-suspended in 25 µl of 5% ACN and analyzed in technical triplicates by time points, injecting 4 µl each into a 6500+ QTrap - Eksigent system (SCIEX™) operating in micro-flow mode. Tryptic peptides were separated using a YMC Triart C18 column as described above. To monitor the system performance, MS Qual/Quant QC Mix, (MRM calibration standard, MSQC1; Sigma-Aldrich) was injected every 15 samples. Two blank runs followed each sample.

Raw MRM data (as.wiff files) were exported to Skyline (MacCoss Lab Software v.19.1) for peak integration, normalization and abundance calculations. Abundance was reported as the ratio between the Aβ17-28 peptide or ¹³C-Lys Aβ17-28 peptide and the ¹³C¹⁵N-Lys Aβ17-28 peptide (global standard). For the brain and lymph nodes, abundance of the Aβ17-28 peptide and ¹³C-Lys Aβ17-28 peptide was additionally normalized to tissue weight. Investigators were blinded to group allocation during all data acquisitions and analyses.

Quantification of Aβ42 levels in peripheral and brain samples

The liver and spleen from mice injected with unlabeled APptg or non-tg brain extracts were homogenized for 1 min. Liver and spleen homogenates (~20–25 mg per sample), and mesenteric lymph nodes were treated with 10 µl of cold 70% FA/mg tissue. Mononuclear blood cell pellets were mixed with 100 µl of cold 70% FA. The samples were processed and Aβ42 levels analyzed as described for brain homogenates. Aβ42 concentrations were calculated as pg Aβ42/mg tissue for tissue samples and normalized to total organ weight and amount of injected Aβ42, yielding percent injected Aβ42. For mononuclear blood cells, Aβ42 concentrations were calculated as pg Aβ42/ml blood. Re-suspended peritoneal cells were treated with two volumes of cold formic acid (minimum of 98%), sonicated for 2 × 30 s on ice, and incubated overnight at 4°C. Peritoneal cell samples were centrifuged at 25,000 × g for 60 min at 4°C. Aβ42 levels were analyzed as described above, calculated as pg Aβ42/500 µl cell suspension, and normalized to amount of injected Aβ42. Blood plasma was assayed for Aβ42 without additional treatment.

Brains from mice injected with unlabeled APptg or non-tg brain extracts were processed as described in detection limit of mass spectrometry methodology. Aβ42 levels were analyzed in the 70% FA fraction from mice injected with ¹³C-Lys APptg or non-tg brain extracts or unlabeled APptg or non-tg brain extracts as described for brain homogenates. Aβ42 concentrations were normalized to protein concentrations measured with a spectrophotometer (ScanDrop, Analytik Jena GmbH, Germany) for samples from mice injected with ¹³C-Lys brain extracts or to brain weight for samples from mice injected with unlabeled brain extracts.

The investigator was blinded to group allocation during all analyses.

Immunohistochemistry

Formalin-fixed hemispheres and segments of livers were embedded in paraffin and sliced on a microtome (4 µm). Slices were stained using a BOND-III automated immunostaining system (Leica Biosystems GmbH, Germany). Coronal brain sections (at approximately –1.4 and –2.5 mm relative to bregma) and liver sections were stained for Aβ (anti-human Aβ clone 4G8; 1:4,000, BioLegend™) as previously described by us (Steffen et al, 2017; Paarmann et al, 2018). Additionally, brain sections were stained for microglia (IBA1, 1:1,000, Wako, 019-19741). After staining, tissue sections were digitized at 230 nm resolution using a Panoramic MidIII slide scanner (3DHistotech, Hungary).

Brain sections were analyzed by an investigator blinded to group allocation, using artificial intelligence in DeePathology STUDIO™ software as previously described by us (Bascuñana et al, 2021; Möhle et al, 2021). Briefly, the software was trained separately to recognize Aβ plaques and activated microglia, respectively. Once the training was completed, stained brain sections were analyzed automatically by DeePathology software after delineating the region of interest including parietal, somatosensory, auditory, and temporal cortices. Results were normalized to 10 mm² cortex area.

Statistical analysis

All statistical analysis was performed using Prism 6 software (GraphPad). Data resulting from Aβ quantification after injection of brain extracts were tested for normality by Kolmogorov–Smirnov test. Normality assumptions were rejected if $P < 0.05$. Unpaired two-tailed *t*-tests were used to compare mass spectrometry, immunoassay, and immunohistochemistry data of ¹³C-Lys APptg extract-injected and ¹³C-Lys non-tg extract-injected groups at each time point after injection. Variance was comparable between groups. Plasma Aβ concentration was analyzed by one-way ANOVA. Levels of unlabeled Aβ in mononuclear blood cells were compared between negative controls and unlabeled APptg extract-injected mice at 1 day after injection by Mann–Whitney *U*-test. Values of $P < 0.05$ were considered statistically significant.

Data availability

All raw and processed data are available at OSF PROP-AD (<http://www.doi.org/10.17605/OSF.IO/VNGPM>). MS data are deposited at: MassIVE MSV000089339 (<https://massive.ucsd.edu/ProteoSAFe/FindDatasets?query=MSV000089339>); www.doi.org/10.25345/C57H1DR1J) and PeptideAtlas PASS01757 (<http://www.peptideatlas.org/PASS/PASS01757>).

Expanded View for this article is available online.

Acknowledgements

We thank Iván Eiriz for skillful assistance with the mouse colonies; Markus Krohn, Luisa Möhle, and Kristin Paarmann for fruitful discussions; Elisabeth Nyberg for establishing early phase measurements of Aβ in non-tg brains; Magdalena Łuczak (IBCh, PAS-Poznan) for sharing her expertise on the MS statistical software and analysis of the MRM data; Jörg A. Gsponer (University of British Columbia, Vancouver, Canada) and Martin Fuhrmann

(Deutsches Zentrum für Neurodegenerative Erkrankungen (DZNE) e.V. Bonn, Germany) for helpful comments on the manuscript.

Funding to J.P. was provided by Deutsche Forschungsgemeinschaft/ Germany (DFG 263024513); HelseSØ/ Norway (2019-054, 2019-055, 2022-046); EEA grant/Norway grants (TAČR TARIMAD TO100078); Norges forskningsråd/ Norway (251290 (PROP-AD), 295910 (PETABC), 327571 (NAPI)).

PROP-AD was supported through the following funding organizations under the aegis of JPND - www.jpnd.eu (AKA #301228 – Finland, BMBF #01ED1605 – Germany, CSO-MOH #30000-12631 – Israel, NFR #260786 – Norway, SRC #2015-06795 – Sweden). PETABC is supported through the following funding organizations under the aegis of JPND - www.jpnd.eu (NFR #327571 – Norway, FFG #882717 – Austria, BMBF #01ED2106 – Germany, MSMT #8F21002 – Czech Republic, VAA #ES RTD/2020/26 – Latvia, ANR #20-JPW2-0002-04 - France, SRC #2020-02905 – Sweden). The projects receive funding from the European Union's Horizon 2020 research and innovation program under grant agreement #643417 (JPco-fuND).

Funding to M.L. was provided by ERA-NET NEURON (ERA-NET Micro-SynDep project); AKA 318857 – Finland.

Funding to AA was provided by Svenska Sällskapet för Medicinsk Forskning (SSMF) (P17-0047), Svenska Forskningsrådet (Formas) (2020-01013), Åke Wiberg stiftelse (M20-0148), Alzheimerfonden (AF-968052), Petrus och Augusta Hedlunds stiftelse (M-2020-1313), Foundation for Geriatric Diseases at Karolinska Institutet (2020-2267), and Åhlén-stiftelsen (203087).

Author contributions

Mirjam Brackhan: Formal analysis; Validation; Investigation; Visualization; Methodology; Writing—original draft; Writing—review and editing. **Giulio Calza:** Formal analysis; Validation; Investigation; Visualization; Methodology. **Kristiina Lundgren:** Investigation; Methodology. **Pablo Bascuñana:** Formal analysis; Investigation; Methodology. **Thomas Brüning:** Investigation; Methodology. **Rabah Soliymani:** Formal analysis; Investigation; Methodology. **Rakesh Kumar:** Investigation; Visualization. **Axel Abelein:** Formal analysis; Investigation; Visualization; Writing—review and editing. **Marc Baumann:** Data curation; Supervision; Validation; Writing—original draft. **Maciej Lalowski:** Formal analysis; Supervision; Validation; Investigation; Visualization; Methodology; Writing—original draft; Writing—review and editing. **Jens Pahnke:** Conceptualization; Resources; Data curation; Formal analysis; Supervision; Funding acquisition; Validation; Investigation; Visualization; Methodology; Writing—original draft; Project administration; Writing—review and editing.

In addition to the CRediT author contributions listed above, the contributions in detail are:

MBr designed and performed mouse experiments, biochemical and molecular analyses, analyzed data, wrote manuscript. GC designed and performed the IP-MALDI-MS, MS^E measurements, established MRM analysis pipelines and analyzed MS data. KL performed the IP-MRM and SILAC experiments. PB performed morphological analyses, wrote manuscript. TB performed tissue processing and analyses. RS provided MS^E and SILAC analysis. RK performed measurements about seeding activity. AA analyzed measurements about seeding activity. MBa provided the MS facility support, provided methodological study discussions. ML designed, supervised, and analyzed MS data, edited manuscript. JP developed the project, acquired the funding, designed experiments, wrote manuscript.

Disclosure and competing interests statement

Jens Pahnke declares competing financial interests related to the publication of this study, including being scientific advisor for DeePathology Ltd., Ra'anana, Israel. Maciej Lalowski is president of the Finnish Proteomics Society and member of the FEBS Fellowships Committee.

References

- Adams HHH, Swanson SA, Hofman A, Arfan Ikram M (2016) Amyloid- β transmission or unexamined bias? *Nature* 537: E7–E9
- Allue JA, Sarasa L, Izco M, Perez-Grijalba V, Fandos N, Pascual-Lucas M, Ogueta S, Pesini P, Sarasa M (2016) Outstanding phenotypic differences in the profile of amyloid-beta between Tg2576 and APPsw/PS1dE9 transgenic mouse models of Alzheimer's disease. *J Alzheimers Dis* 53: 773–785
- Asher DM, Belay E, Bigio E, Brandner S, Brubaker SA, Caughey B, Clark B, Damon I, Diamond M, Freund M *et al* (2020) Risk of transmissibility from neurodegenerative disease-associated proteins: experimental knowns and unknowns. *J Neuropathol Exp Neurol* 79: 1141–1146
- Bascuñana P, Brackhan M, Pahnke J (2021) Machine learning-supported analyses improve quantitative histological assessments of amyloid- β deposits and activated microglia. *J Alzheimers Dis* 79: 597–605
- Bateman RJ, Munsell LY, Morris JC, Swarm R, Yarasheski KE, Holtzman DM (2006) Human amyloid-beta synthesis and clearance rates as measured in cerebrospinal fluid *in vivo*. *Nat Med* 12: 856–861
- Bu X-L, Xiang Y, Jin W-S, Wang J, Shen L-L, Huang Z-L, Zhang K, Liu Y-H, Zeng F, Liu J-H *et al* (2018) Blood-derived amyloid- β protein induces Alzheimer's disease pathologies. *Mol Psychiatry* 23: 1948–1956
- Burwinkel M, Lutzenberger M, Heppner FL, Schulz-Schaeffer W, Baier M (2018) Intravenous injection of beta-amyloid seeds promotes cerebral amyloid angiopathy (CAA). *Acta Neuropathol Commun* 6: 23
- Cali I, Cohen ML, Häik S, Parchi P, Giaccone G, Collins SJ, Kofsky D, Wang H, McLean CA, Brandel J-P *et al* (2018) Iatrogenic Creutzfeldt-Jakob disease with Amyloid- β pathology: an international study. *Acta Neuropathol Commun* 6: 5
- Cohen SIA, Linse S, Luheshi LM, Hellstrand E, White DA, Rajah L, Otzen DE, Vendruscolo M, Dobson CM, Knowles TPJ (2013) Proliferation of amyloid- β 42 aggregates occurs through a secondary nucleation mechanism. *Proc Natl Acad Sci USA* 110: 9758–9763
- Duyckaerts C, Sazdovitch V, Ando K, Seilhean D, Privat N, Yilmaz Z, Peckeu L, Amar E, Comoy E, Maceski A *et al* (2018) Neuropathology of iatrogenic Creutzfeldt-Jakob disease and immunoassay of French cadaver-sourced growth hormone batches suggest possible transmission of tauopathy and long incubation periods for the transmission of Abeta pathology. *Acta Neuropathol* 135: 201–212
- Eisele YS (2013) From soluble A β to progressive A β aggregation: could prion-like templated misfolding play a role? *Brain Pathol* 23: 333–341
- Eisele YS, Obermuller U, Heilbronner G, Baumann F, Kaeser SA, Wolburg H, Walker LC, Staufienbiel M, Heikenwalder M, Jucker M (2010) Peripherally applied Abeta-containing inoculates induce cerebral beta-amyloidosis. *Science* 330: 980–982
- Eisele YS, Fritschi SK, Hamaguchi T, Obermuller U, Fuger P, Skodras A, Schafer C, Odenthal J, Heikenwalder M, Staufienbiel M *et al* (2014) Multiple factors contribute to the peripheral induction of cerebral beta-amyloidosis. *J Neurosci* 34: 10264–10273
- Feeny C, Scott GP, Cole JH, Sastre M, Goldstone AP, Leech R (2016) Seeds of neuroendocrine doubt. *Nature* 535: E1–E2
- Gholizadeh E, Karbalaee R, Khaleghian A, Salimi M, Gilany K, Soliymani R, Tanoli Z, Rezadoost H, Baumann M, Jafari M *et al* (2021) Identification of celecoxib-targeted proteins using label-free thermal proteome profiling on rat hippocampus. *Mol Pharmacol* 99: 308–318
- Hardy JA, Higgins GA (1992) Alzheimer's disease: the amyloid cascade hypothesis. *Science* 256: 184–185
- Huynh TV, Holtzman DM (2018) Amyloid- β 'seeds' in old vials of growth hormone. *Nature* 564: 354–355

- Irwin DJ, Abrams JY, Schonberger LB, Leschek EW, Mills JL, Lee VM, Trojanowski JQ (2013) Evaluation of potential infectivity of Alzheimer and Parkinson disease proteins in recipients of cadaver-derived human growth hormone. *JAMA Neurol* 70: 462–468
- Jaunmuktane Z, Mead S, Ellis M, Wadsworth JDF, Nicoll AJ, Kenny J, Launchbury F, Linehan J, Richard-Loendt A, Walker AS et al (2015) Evidence for human transmission of amyloid- β pathology and cerebral amyloid angiopathy. *Nature* 525: 247–250
- Jucker M, Walker LC (2013) Self-propagation of pathogenic protein aggregates in neurodegenerative diseases. *Nature* 501: 45–51
- Jucker M, Walker LC (2015) Amyloid- β pathology induced in humans. *Nature* 525: 193–194
- Kawarabayashi T, Younkin LH, Saido TC, Shoji M, Ashe KH, Younkin SG (2001) Age-dependent changes in brain, CSF, and plasma amyloid (beta) protein in the Tg2576 transgenic mouse model of Alzheimer's disease. *J Neurosci* 21: 372–381
- Kim JS, Ahn HS, Cho SM, Lee JE, Kim Y, Lee C (2014) Detection and quantification of plasma amyloid- β by selected reaction monitoring mass spectrometry. *Anal Chim Acta* 840: 1–9
- Kollmer M, Close W, Funk L, Rasmussen J, Bsoul A, Schierhorn A, Schmidt M, Sigurdson CJ, Jucker M, Fändrich M (2019) Cryo-EM structure and polymorphism of A β amyloid fibrils purified from Alzheimer's brain tissue. *Nat Commun* 10: 4760
- Krüger M, Moser M, Ussar S, Thievensen I, Lubert CA, Forner F, Schmidt S, Zanivan S, Fässler R, Mann M (2008) SILAC mouse for quantitative proteomics uncovers kindlin-3 as an essential factor for red blood cell function. *Cell* 134: 353–364
- Lau HHC, Ingelsson M, Watts JC (2021) The existence of A β strains and their potential for driving phenotypic heterogeneity in Alzheimer's disease. *Acta Neuropathol* 142: 17–39
- Lauwers E, Lalli G, Brandner S, Collinge J, Compennolle V, Duyckaerts C, Edgren G, Haik S, Hardy J, Helmy A et al (2020) Potential human transmission of amyloid β pathology: surveillance and risks. *Lancet Neurol* 19: 872–878
- Meisl G, Yang X, Hellstrand E, Frohm B, Kirkegaard JB, Cohen SIA, Dobson CM, Linse S, Knowles TPJ (2014) Differences in nucleation behavior underlie the contrasting aggregation kinetics of the A β 40 and A β 42 peptides. *Proc Natl Acad Sci USA* 111: 9384–9389
- Michno W, Stringer KM, Enzlein T, Passarelli MK, Escrig S, Vitanova K, Wood J, Blennow K, Zetterberg H, Meibom A et al (2021) Following spatial A β aggregation dynamics in evolving Alzheimer's disease pathology by imaging stable isotope labeling kinetics. *Sci Adv* 7: eabg4855
- Möhle L, Bascuñana P, Brackhan M, Pahnke J (2021) Development of deep learning models for microglia analyses in brain tissue using DeePathology™ STUDIO. *J Neurosci Methods* 364: 109371. <https://doi.org/10.1016/j.jneumeth.2021.109371>
- Morales R, Duran-Aniotz C, Bravo-Alegria J, Estrada LD, Shahnawaz M, Hu PP, Kramm C, Morales-Scheihing D, Urayama A, Soto C (2020) Infusion of blood from mice displaying cerebral amyloidosis accelerates amyloid pathology in animal models of Alzheimer's disease. *Acta Neuropathol Commun* 8: 213
- Morales R, Bravo-Alegria J, Moreno-Gonzalez I, Duran-Aniotz C, Gamez N, Edwards Iii G, Soto C (2021) Transmission of cerebral amyloid pathology by peripheral administration of misfolded A β aggregates. *Mol Psychiatry* 26: 5690–5701
- Paarmann K, Prakash SR, Krohn M, Möhle L, Brackhan M, Brüning T, Eiriz I, Pahnke J (2019) French maritime pine bark treatment decelerates plaque development and improves spatial memory in Alzheimer's disease mice. *Phytomedicine* 57: 39–48
- Price JC, Guan S, Burlingame A, Prusiner SB, Ghaemmaghami S (2010) Analysis of proteome dynamics in the mouse brain. *Proc Natl Acad Sci USA* 107: 14508–14513
- Purro SA, Farrow MA, Linehan J, Nazari T, Thomas DX, Chen Z, Mengel D, Saito T, Saido T, Rudge P et al (2018) Transmission of amyloid- β protein pathology from cadaveric pituitary growth hormone. *Nature* 564: 415–419
- Radde R, Bolmont T, Kaeser SA, Coomaraswamy J, Lindau D, Stoltze L, Calhoun ME, Jäggi F, Wolburg H, Gengler S et al (2006) A β 42-driven cerebral amyloidosis in transgenic mice reveals early and robust pathology. *EMBO Rep* 7: 940–946
- Ritchie DL, Adlard P, Peden AH, Lowrie S, Le Grice M, Burns K, Jackson RJ, Yull H, Keogh MJ, Wei W et al (2017) Amyloid-beta accumulation in the CNS in human growth hormone recipients in the UK. *Acta Neuropathol* 134: 221–240
- Sagare A, Deane R, Bell RD, Johnson B, Hamm K, Pendu R, Marky A, Lenting PJ, Wu Z, Zarcone T et al (2007) Clearance of amyloid-beta by circulating lipoprotein receptors. *Nat Med* 13: 1029–1031
- Selkoe DJ (2001) Alzheimer's disease: genes, proteins, and therapy. *Physiol Rev* 81: 741–766
- Steffen J, Krohn M, Schwitlick C, Brüning T, Paarmann K, Pietrzik CU, Biverstäl H, Jansone B, Langer O, Pahnke J (2017) Expression of endogenous mouse APP modulates β -amyloid deposition in hAPP-transgenic mice. *Acta Neuropathol Commun* 5: 49. <https://doi.org/10.1186/s40478-017-0448-2>
- Sturchler-Pierrat C, Abramowski D, Duke M, Wiederhold KH, Mistl C, Rothacher S, Ledermann B, Bürki K, Frey P, Paganetti PA et al (1997) Two amyloid precursor protein transgenic mouse models with Alzheimer disease-like pathology. *Proc Natl Acad Sci USA* 94: 13287–13292
- Villeda SA, Luo J, Mosher KI, Zou B, Britschgi M, Bieri G, Stan TM, Fainberg N, Ding Z, Eggel A et al (2011) The ageing systemic milieu negatively regulates neurogenesis and cognitive function. *Nature* 477: 90–94
- Wendeln A-C, Degenhardt K, Kaurani L, Gertig M, Ulas T, Jain G, Wagner J, Häslér LM, Wild K, Skodras A et al (2018) Innate immune memory in the brain shapes neurological disease hallmarks. *Nature* 556: 332–338
- Wildburger NC, Gyngard F, Guillemier C, Patterson BW, Elbert D, Mawuenyega KG, Schneider T, Green K, Roth R, Schmidt RE et al (2018) Amyloid-beta plaques in clinical Alzheimer's disease brain incorporate stable isotope tracer *in vivo* and exhibit nanoscale heterogeneity. *Front Neurol* 9: 169
- Yang AC, Stevens MY, Chen MB, Lee DP, Stähli D, Gate D, Contrepois K, Chen W, Iram T, Zhang L et al (2020) Physiological blood-brain transport is impaired with age by a shift in transcytosis. *Nature* 583: 425–430
- Yoo S, Zhang S, Kreutzer AG, Nowick JS (2018) An efficient method for the expression and purification of A β (M1-42). *Biochemistry* 57: 3861–3866



License: This is an open access article under the terms of the Creative Commons Attribution-NonCommercial-NoDerivs License, which permits use and distribution in any medium, provided the original work is properly cited, the use is non-commercial and no modifications or adaptations are made.